Analysis of experiment matched "omic" datasets highlight the importance of viewing RNA, protein, and metabolite data together to explain the processes that change during the cell cycle.

Abundances of transcripts, proteins, and metabolites in the cell cycle of budding yeast reveal coordinate control of lipid metabolism

Heidi M. Blank[a], Ophelia Papoulas[b,c], Nairita Maitra[a], Riddhiman Garge[b,c], Birgit Schilling[f], Edward M. Marcotte[b,c,*], and Michael Polymenis[a,*]

[a]Department of Biochemistry and Biophysics, Texas A&M University, College Station, TX 77843; [b]Center for Systems and Synthetic Biology and [c]Department of Molecular Biosciences, University of Texas at Austin, Austin, TX 78712; [d]Departments of Biochemistry and Physiology, Yong Loo Lin School of Medicine, National University of Singapore, Singapore 117596; [e]Centre for Healthy Ageing, National University of Singapore, National University Health System, Singapore 117609; [f]Buck Institute for Research on Aging, Novato, CA 94945

ABSTRACT Establishing the pattern of abundance of molecules of interest during cell division has been a long-standing goal of cell cycle studies. Here, for the first time in any system, we present experiment-matched datasets of the levels of RNAs, proteins, metabolites, and lipids from unarrested, growing, and synchronously dividing yeast cells. Overall, transcript and protein levels were correlated, but specific processes that appeared to change at the RNA level (e.g., ribosome biogenesis) did not do so at the protein level, and vice versa. We also found no significant changes in codon usage or the ribosome content during the cell cycle. We describe an unexpected mitotic peak in the abundance of ergosterol and thiamine biosynthesis enzymes. Although the levels of several metabolites changed in the cell cycle, by far the most significant changes were in the lipid repertoire, with phospholipids and triglyc- erides peaking strongly late in the cell cycle. Our findings provide an integrated view of the abundance of biomolecules in the eukaryotic cell cycle and point to a coordinate mitotic control of lipid metabolism.

INTRODUCTION Identifying biomolecules that change levels during the cell cycle has been a critical objective for decades to understand how cell division processes are integrated. Much work has been published with regards to changes in mRNA levels, but less so at the protein and metbolite level. For the first time, **we use synchronized, unarrested budding yeast cells to generate datasets for RNAs, proteins, metabolites, and lipids from the same set of cells progressing through the cell cycle.**

Experimental design.

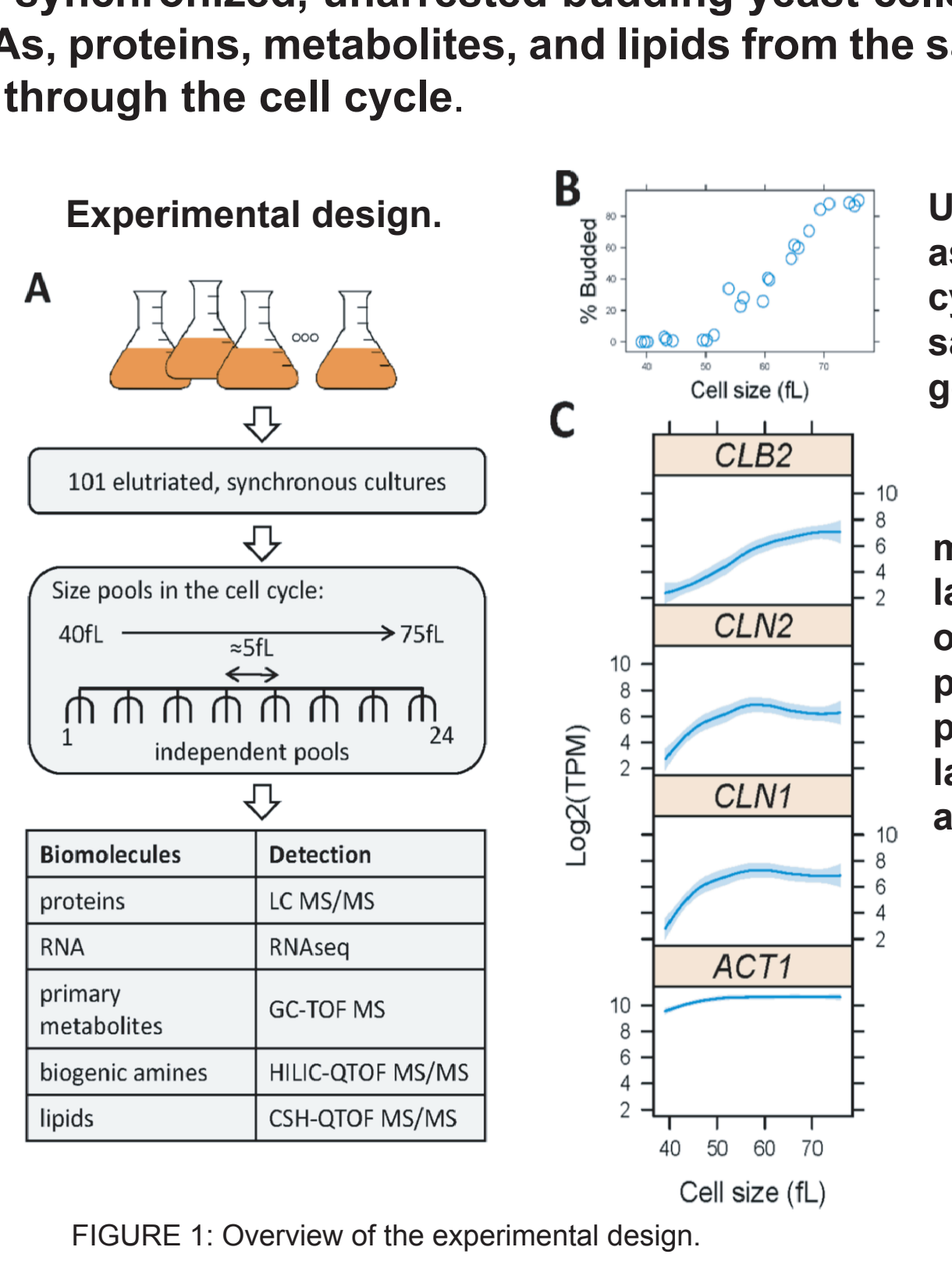

A
101 elutriated, synchronous cultures
Size pools in the cell cycle:
40fL
75fL
≈5fL
1
24
independent pools
Biomolecules
Detection
proteins
LC MS/MS
RNA
RNAseq
primary metabolites
GC-TOF MS
biogenic amines
HILIC-QTOF MS/MS
lipids
CSH-QTOF MS/MS
B
% Budded
Cell size (fL)
C
CLB2
CLN2
CLN1
ACT1
Log2(TPM)
Cell size (fL)

Using budding index as a marker for cell cycle progression, the sample size series had good synchrony.

mRNAs known to oscillate were also found in our experiment. Compare the top three panels to the non-oscillatory ACT1, encoding actin.

FIGURE 1: Overview of the experimental design.

DATA / RESULTS

Heatmap of 652 differentially expressed transcripts

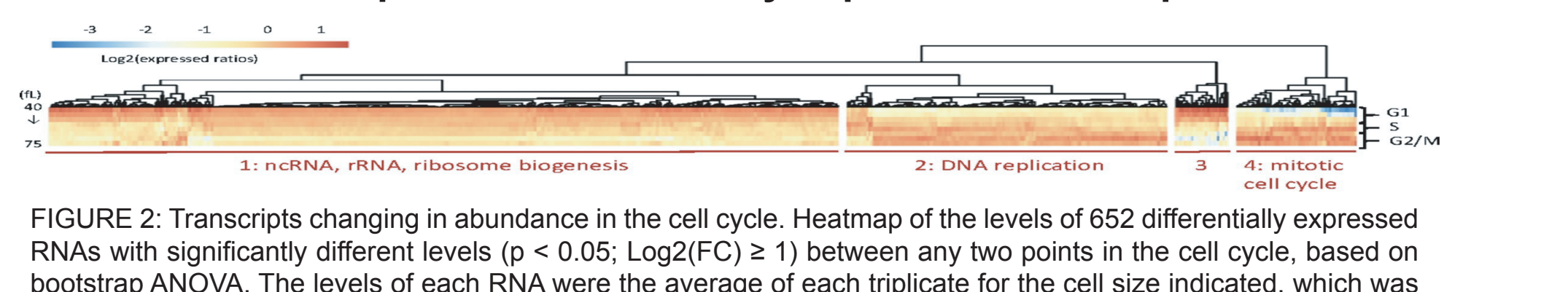

FIGURE 2: Transcripts changing in abundance in the cell cycle. Heatmap of the levels of 652 differentially expressed RNAs with significantly different levels ($p < 0.05$; Log2(FC) ≥ 1) between any two points in the cell cycle, based on bootstrap ANOVA. The levels of each RNA were the average of each triplicate for the cell size indicated, which was then divided by the average value of the entire cell size series for that RNA. These expressed ratios were then Log2-transformed. The Log2(expressed ratios) values were hierarchically clustered and displayed with the pheatmap R language package.

Overall, protein and mRNA levels were correlated, and 333 proteins were identified whose abundance changed significantly throughout the cell cycle.

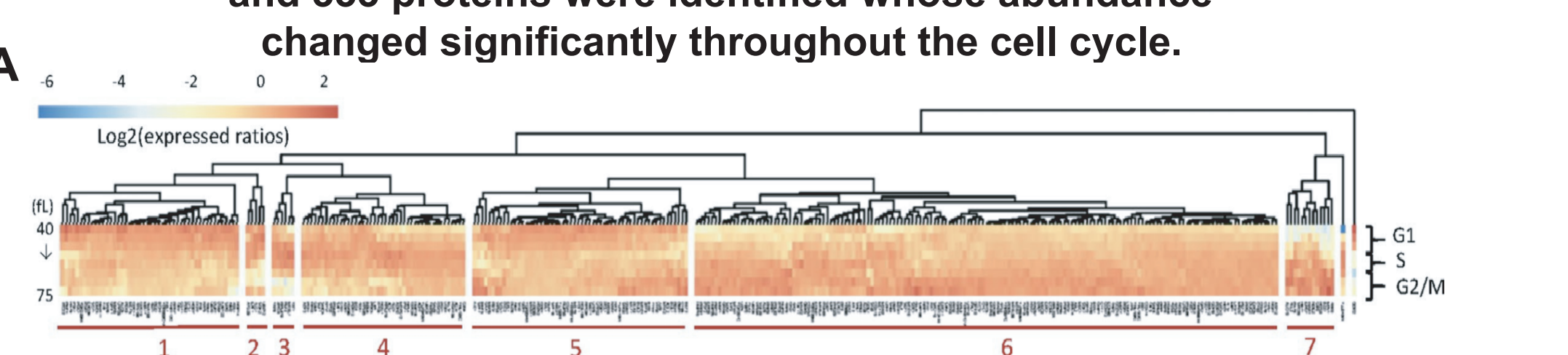

FIGURE 3: (A) Heatmap displaying the relative abundance of the 333 proteins, generated as in Figure 2.

However, there were groups of proteins whose mRNA and protein abundance did not correlate.

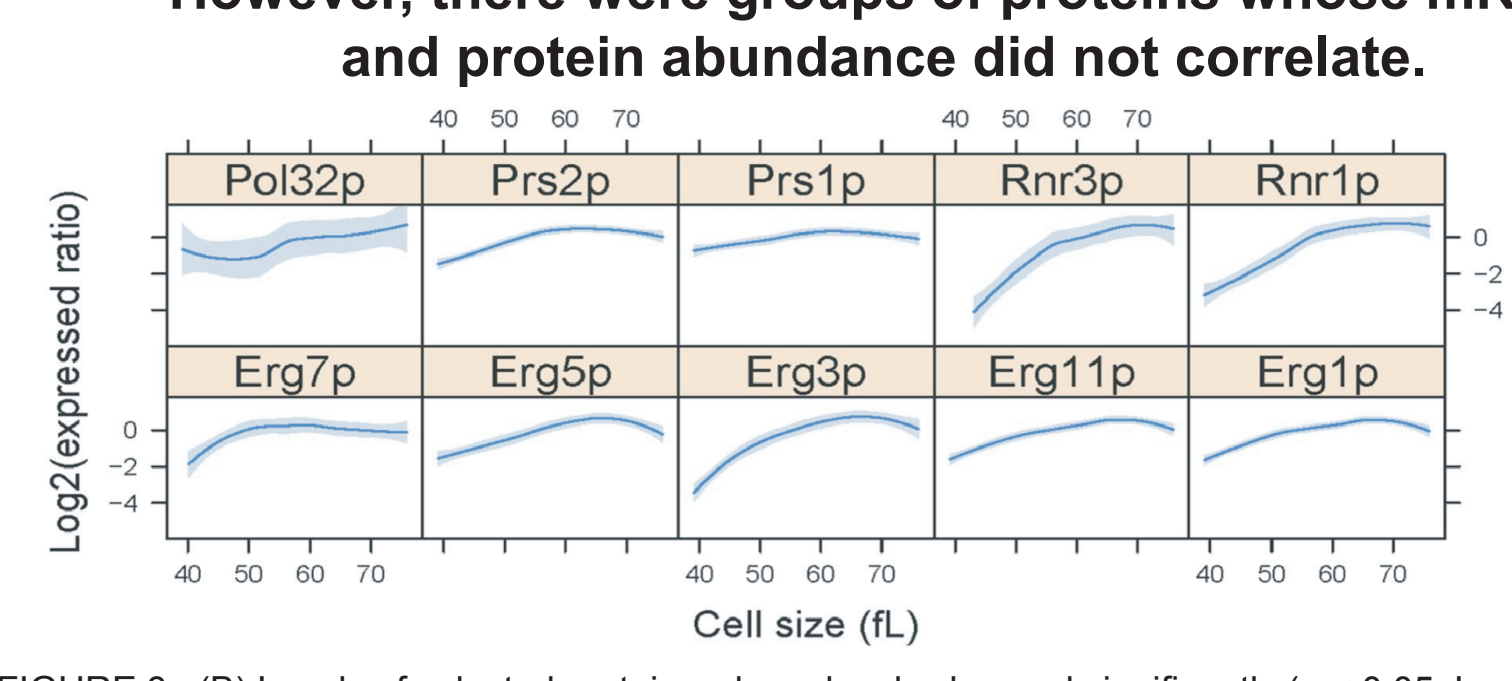

DNA metabolism mRNA ~ protein

ergosterol biosynthesis mRNA ≠ protein

FIGURE 3: (B) Levels of selected proteins whose levels changed significantly ($p < 0.05$; Log2(FC) ≥ 1) between any two points in the cell cycle. Top, enzymes involved in DNA metabolism (Pol32p: DNA polymerase δ; Prs1,2p: PRPP synthase; Rnr1,3p: ribonucleoside-diphosphate reductase).ergosterol biosynthesis. Bottom, enzymes involved in ergosterol biosynthesis The corresponding Log2(expressed ratios) values from all 24 data points are on the y-axis, and cell size values are on the x-axis. Loess curves and confidence bands indicating the standard errors on the curve at a 0.95 level are shown.

Ribosomal proteins were another class of protein whose abundance did NOT match the G1 upregulation seen with transcription. Ribosome composition was unaltered during the cell cycle as well.

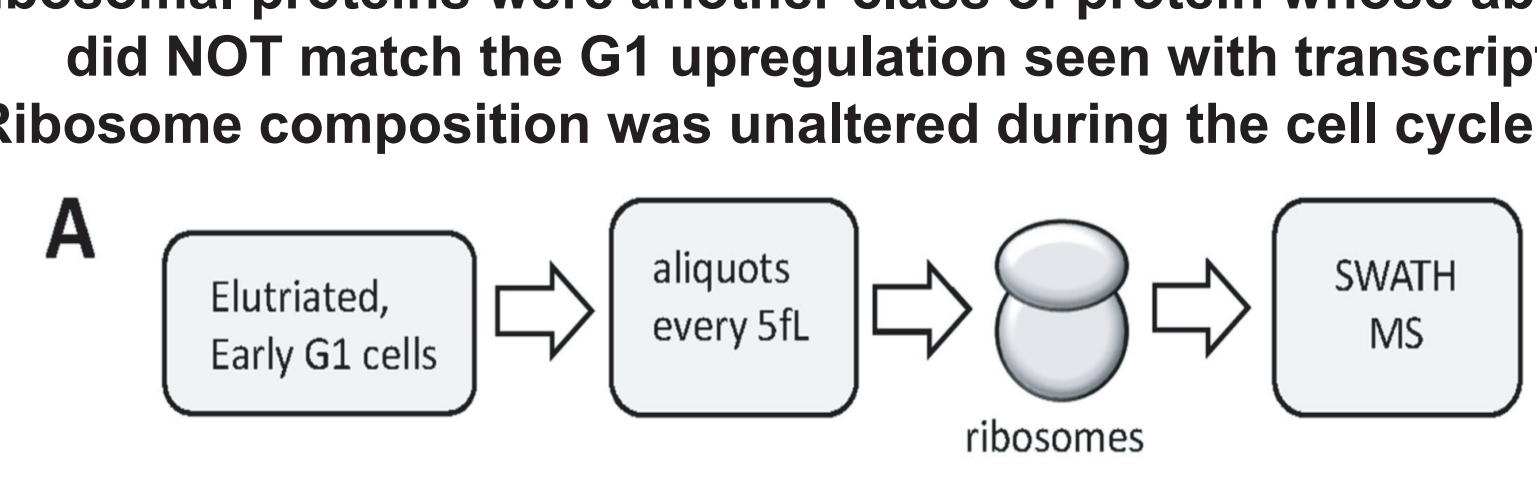

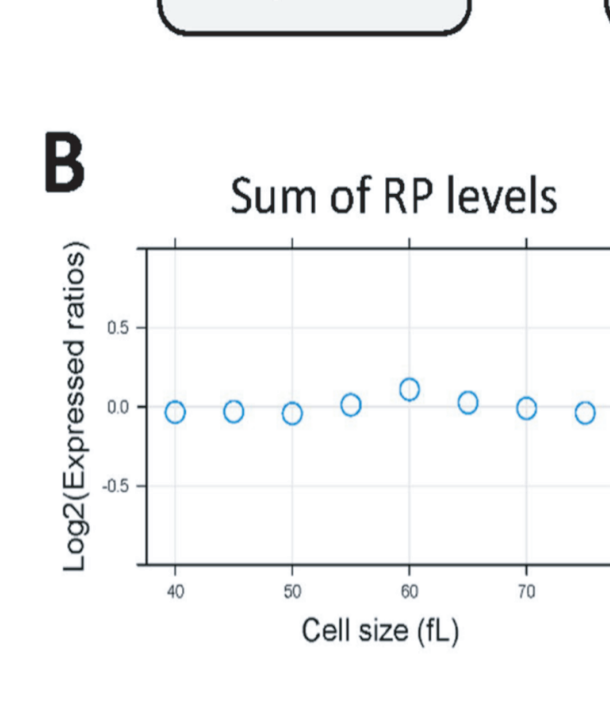

C

RP composition - correlations

	40fL	45fL	50fL	55fL	60fL	65fL	70fL	75fL
40fL	1	1	0.99	0.99	0.99	0.99	0.99	0.99
45fL	1	1	1	0.99	0.99	0.99	0.99	0.99
50fL	0.99	1	1	0.99	0.99	0.99	1	0.99
55fL	0.99	0.99	0.99	1	0.98	0.98	0.98	0.99
60fL	0.99	0.99	0.99	0.98	1	1	0.99	0.99
65fL	0.99	0.99	0.99	0.98	1	1	1	1
70fL	0.99	0.99	1	0.98	0.99	1	1	1
75fL	0.99	0.99	0.99	0.99	0.99	1	1	1

FIGURE 4: Ribosomal protein abundance in ribosomes does not change in the cell cycle. (A) Elutriated, early G1 cells were cultured, and sampled at regular intervals in the cell cycle, in three biological replicates at each 5 fL range, from 40 to 75 fL. Protein extracts from the same number of cells were then fractionated by sucrose ultracentrifugation, to isolate ribosomes on mRNAs, which were then analyzed by SWATH-MS. (B) The peak areas corresponding to each ribosomal protein (RP) detected were summed and averaged across the triplicate for each cell size interval. The Log2(expressed ratios) values for the Sum of RP levels are shown on the y-axis, while cell size is on the x-axis. (C) Correlation matrix of the relative abundance of individual ribosomal proteins in assembled ribosomes on mRNAs. The Spearman correlation coefficients (ρ) shown in each case were calculated with the rcorr function of the Hmisc R language package.

Because we had stringent statistical cutoffs, we searched for proteins whose levels varied highly throughout the cell cycle, but were not identified through our computational analysis.

Thiamine diphosphate (TDP) biosysnthesis enzymes peaked late in the cell cycle.

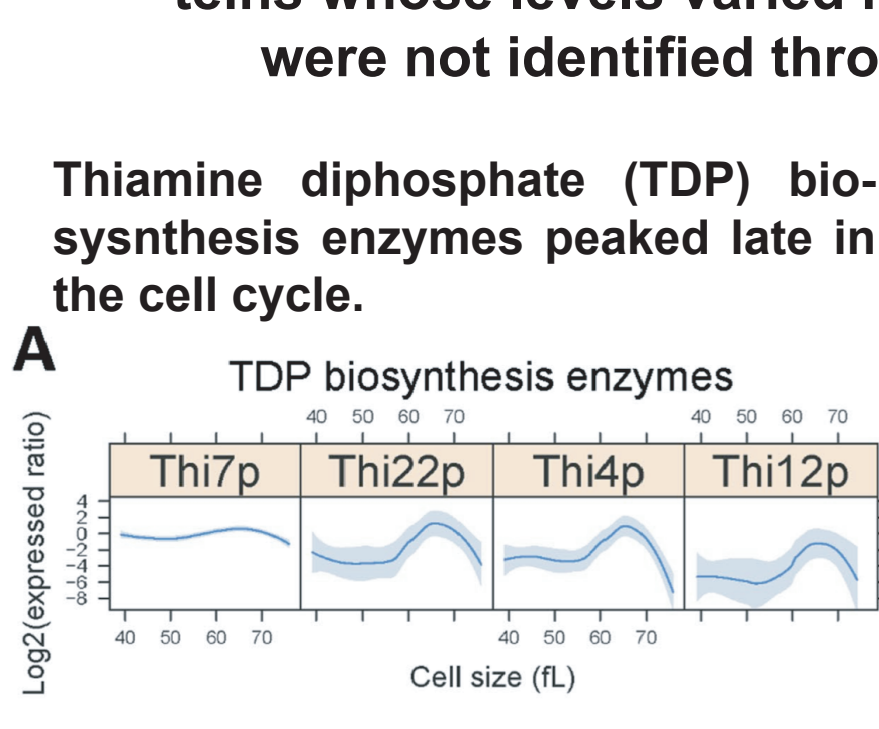

Results from (A) were verified by elutriation and immunoblotting.

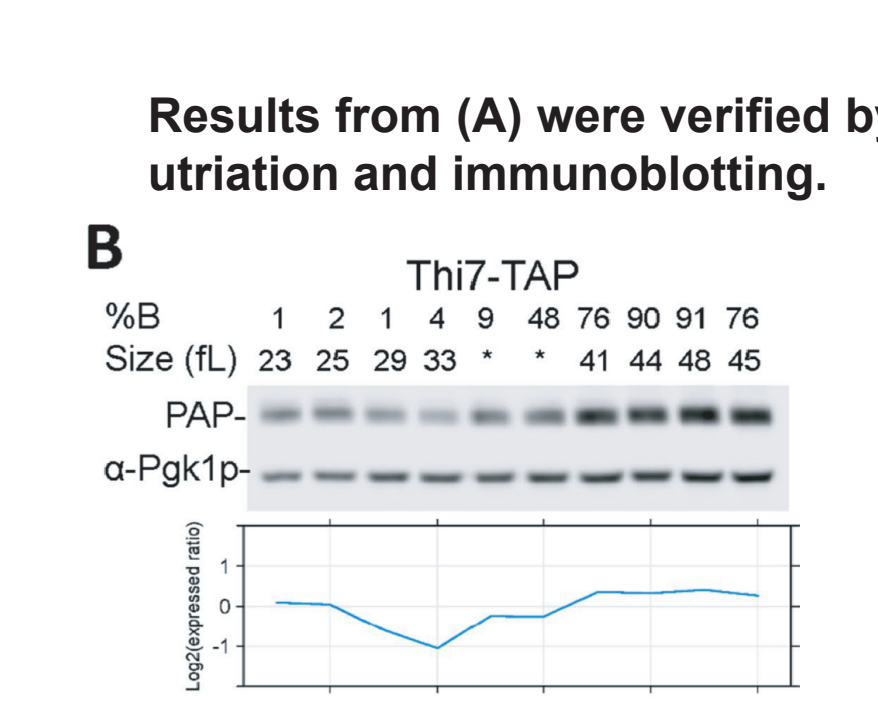

Levels of three TDP-dependent enzymes also change in the cell cycle.

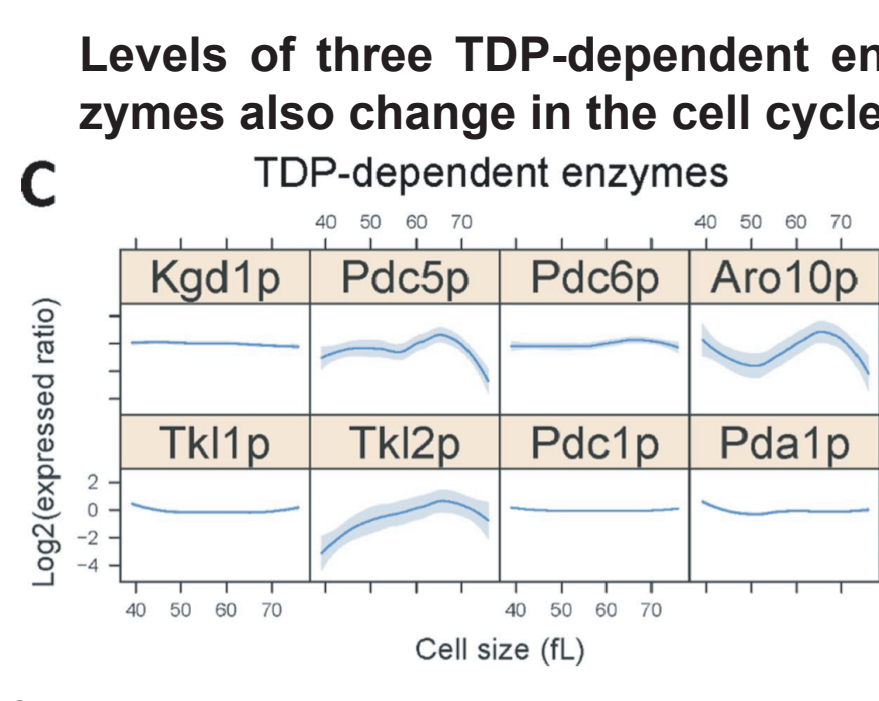

Deletion of a TDP-dependent enzyme changes cell size, possibly altering cell cycle progression.

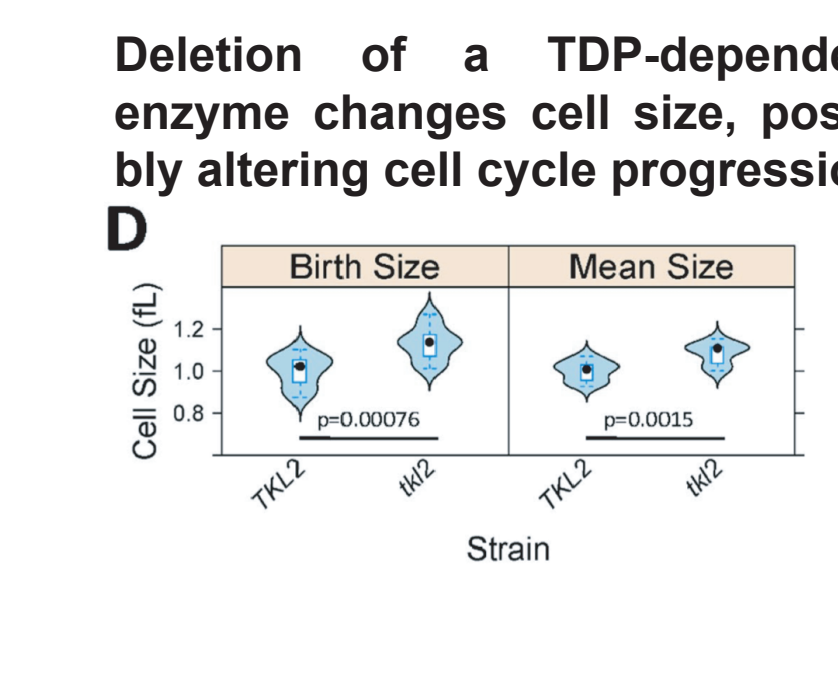

FIGURE 5: Thiamine biosynthesis and TDP-dependent enzymes in the cell cycle. (A) Abundances of the indicated proteins of thiamine biosynthesis from LC-MS/MS, across the cell size series (x-axis, in fL). The corresponding Log2(expressed ratios) values from all 24 data points are on the y-axis. Loess curves and confidence bands indicating the standard errors on the curve at a 0.95 level were drawn using the default settings of the panel.smoother function of the latticeExtra R language package. (B) The abundance of Thi7-TAP by immunoblotting from synchronous, elutriated cells, progressing in the cell cycle and sampled at regular intervals, as indicated (%B is the percentage of budded cells; fL is the cell size). Pgk1p levels are also shown from the same samples, to indicate loading. For the two samples indicated with an asterisk in the Thi7-TAP series, there were no size data due to instrument malfunction. At the bottom, the band intensities were quantified with ImageJ software, and the Log2-transformed expressed ratios of Thi7-TAP are shown, after they were normalized against Pgk1p. (C) Abundances of the indicated TDP-dependent proteins are determined and displayed as in A. (D) The birth and mean size of tkl2 cells and experiment-matched wild-type (TKL2) cultures from exponentially dividing cells in rich, undefined media (YPD). At least 12 independent cultures were measured in each case. Significant differences and the associated p values were indicated by the nonparametric Wilcoxon rank sum test, performed with the wilcox.test function of the R stats package.

406 primary metabolites, biogenic amines, and complex lipids were identified from the same samples used to analyze RNAs and proteins.

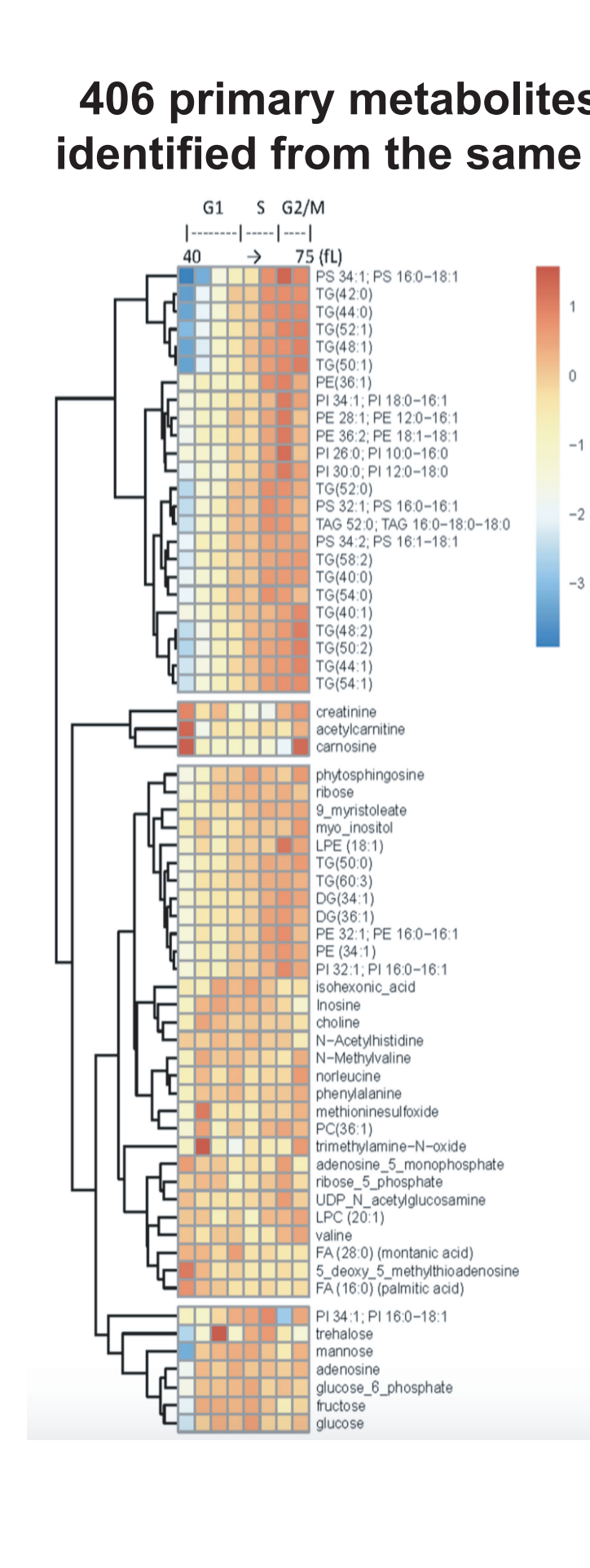

G1
S
G2/M
40
75 (fL)
Log2(expressed ratios)
creatinine
acetylcarnitine
carnosine
phytosphingosine
ribose
myo_inositol
isohexonic_acid
Inosine
choline
N-Acetylhistidine
N-Methylvaline
norleucine
phenylalanine
methioninesulfoxide
trimethylamine-N-oxide
adenosine_5_monophosphate
ribose_5_phosphate
UDP_N_acetylglucosamine
valine
trehalose
mannose
adenosine
glucose_6_phosphate
fructose
glucose

- **Lipids were the most upregulated class of molecules, peaking late in the cell cycle.**
- **Trehalose (a storage carbohydrate) rises in G1, then falls.**
- **Gycolysis is up-regulated before DNA replication, as seen by high levels of glucose, fructose, mannose, and glucose-6-phosphate in G1.**

FIGURE 6: Lipid levels change significantly in the cell cycle. (A) From 406 known metabolites identified from all classes (primary, biogenic amines, complex lipids), the levels of 64 with significantly different levels ($p < 0.05$; Log2(FC) ≥ 1) between any two points in the cell cycle, based on bootstrap ANOVA, are shown in theheatmap. The levels of each metabolite were the average of each triplicate for the cell size indicated, which was then divided by the average value of the entire cell size series for that metabolite. These expressed ratios were then Log2-transformed. The Log2(expressed ratios) values were hierarchically clustered and displayed with the pheatmap R language package. The different columns of the heatmap correspond to the different cell sizes (40–75 fL, left to right, in 5-fL intervals).

DISCUSSION / SUMMARY

Same sample set

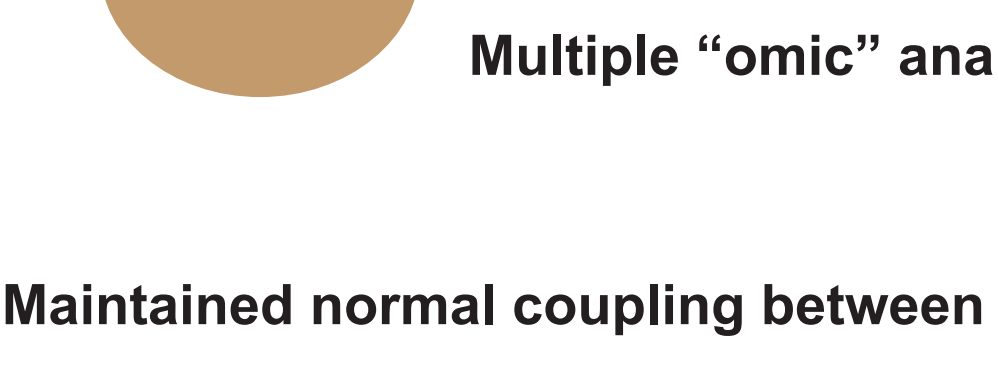

Multiple "omic" analysis

RNAs
Proteins
Meabolites
Biogenic amines
Lipids

- **Maintained normal coupling between cell division and growth.**
- **The transcriptome and proteome were highly correlated, but there were clear groups that did not fit this pattern.**

Ribosomal synthesis-strong G1 transcriptional wave but constant at the protein level.

Ribosome content is also constant during the cell cycle.

Ergosterol biosynthetic enzymes peak in mitosis, despite no change in their transcript. This is a new finding, and significant in the context of the mitotic lipid peak we saw in the metabolite analysis. These enzymes levels may be controlled by regulated proteolysis, since they have shown to be ubiqinated, but further work will have to be done.

TDP biosynthetic enzymes peak in mitosis, despite no change in their transcripts.

TDP-dependent transketolase activity necessary for mouse oocyte meiotic progression.

Loss of Tkl2p increased cell size, but the mechanism for this remains unclear.

- **Lipid levels (especially phospholipids and triglycerides) increase at mitosis, consistent with other studies linking lipid metabolism and mitotic entry.**
- **Our comprehensive cell cycle analysis is consistent with previous studies, validating our experimental method, and builds on the existing knowledge. Integrating multiple "omic" datasets greatly increases the chance of identifying relevant cellular responses that might otherwise be missed.**

MATERIALS AND METHODS

For more details, methods, and supplemental data and figures, please visit MBoC in Press at http://www.molbiol-cell.org/cgi/doi/10.1091/mbc.E19-12-0708.